

# **IMPROVEMENT OF PORCELAIN TILE PROPERTIES BY USING FRITS IN THE BODY COMPOSITION**

**Moreno, J. García-Ten, F. Quereda, V. Sanz**

Instituto de Tecnología Cerámica (ITC)  
Asociación de Investigación de las Industrias Cerámicas (AICE)  
Universitat Jaume I. Castellón. España

**J. Manrique, J. García-Sainz, J. Bort**

Ferro Enamel Española, S.A.

## **1. INTRODUCTION**

Porcelain tile manufacture has undergone considerable aesthetic development in recent years, complementing the product's excellent technical characteristics. Most of the implemented decorating techniques, some of which have been specifically designed for porcelain tile, are based on colouring the body mass, which means that the body needs to have the appropriate colour development capability.

The present work was undertaken to study the feasibility of using frits of different nature (transparent, matt, etc.) as admixtures in porcelain tile compositions to improve certain product characteristics.

## **2. OBJECTIVE AND SCOPE**

The present study was designed to determine the feasibility of incorporating frits into porcelain tile compositions as fluxes, while enhancing porcelain tile whiteness and colour development.

A wide range of frits was initially considered for this purpose and after performing certain preliminary tests, the most promising frits were selected to attempt to improve the above properties. The mechanisms that allowed the selected frits to provide the porcelain tiles with meltability, enhanced whiteness and colour development were then studied in greater detail.

### 3. EXPERIMENTAL

#### 3.1.- MATERIALS

The study was conducted with a standard industrial spray-dried powder employed for porcelain tile manufacture (STD), whose chemical analysis is presented in Table 1, and a set of frits of different nature. The following frits were tested:

—Frits for developing compositions with high meltability:

- Frit A. High-temperature, boron-free, glossy single-fire frit.
- Frit B. Boron-free, fluxing alkali frit.
- Frit C. Lithium-containing fluxing frit.

—Frits for developing compositions with high whiteness:

◆ Zirconium-containing frits

- Frit D. High-temperature, boron-free, glossy single-fire frit.
- Frit E. Titanium-containing, glossy opaque frit.
- Frit F. Titanium-containing, opaque matt frit.
- Frit G. Barium and zinc-containing, semi-glossy, matt frit.

◆ Zirconium-free frits

- Frit H. Calcium and magnesium-containing matt frit.
- Frit I. Titanium-containing matt frit.
- Frit J. High-temperature, barium-containing matt frit.

Oxide	SiO <sub>2</sub>	Al <sub>2</sub> O <sub>3</sub>	Fe <sub>2</sub> O <sub>3</sub>	CaO	MgO	Na <sub>2</sub> O	K <sub>2</sub> O	TiO <sub>2</sub>	L.O.I.
wt%	67.7	20.1	0.62	0.63	0.23	4.28	1.41	0.87	4.05

**Table 1.** Chemical compositions of the industrial spray-dried powder (STD)

#### 3.2.- EXPERIMENTAL PROCEDURE

##### *Composition preparation*

The study was conducted on compositions prepared by adding 6 wt% of each frit to the spray-dried powder. This was done by wet mixing the porcelain tile composition with the corresponding frits milled to a reject of around 4% on a 40- $\mu$ m-mesh screen. The resulting suspensions were dried under infrared lamps. The reference assigned to each

mixture consists of two letters: the first, C, indicates that a composition is involved, and the second varies according to the added frit.

#### *Vitrification diagram*

To obtain the vitrification diagrams, cylindrical test specimens were made (about 6 mm thick, with a 40-mm diameter) by uniaxial pressing at a moisture content of 5.5%, using the pressure required to produce a dry bulk density of 1.91 g/cm<sup>3</sup>. This was done by previously preparing the compaction diagrams.

The test specimens were dried at 110°C in an electric laboratory oven with recirculating air to constant weight. The specimens were then weighed, their diameter was measured and bulk density was determined by the mercury immersion method.

After drying, the test specimens were fired in an electric laboratory kiln at different peak temperatures with a fast-firing cycle and a 6-min hold at peak temperature. The heating rate was 25°C/min, cooling by forced convection.

After firing the specimens were reweighed, determining bulk density as above. Linear shrinkage was calculated from the dry and fired diameter data, and water absorption was found by measuring specimen weight gain after immersion for two hours in boiling water.

#### *Chromatic coordinates*

The chromatic coordinates ( $L^*$ ,  $a^*$ ,  $b^*$ ) were determined on a diffuse reflectance spectrophotometer using a D<sub>65</sub> type illuminant and standard observer at 10°.

#### *Melting test*

The melting test was run on a MISURA hot-stage microscope. The hot-stage microscope is an instrument that enables visualising a sample and recording the silhouette as the sample undergoes heat-treatment. The recorded images then permit determining how sample shrinkage evolves with temperature by means of an image analyser.

#### *Identification of crystalline phases*

The crystalline phases present in the fired specimens were identified on a Philips, X'Pert X-ray diffraction instrument, comparing the diffractograms with the JCPDS files for pure crystalline phases.

#### *Microstructure observation and energy-dispersive X-ray analysis*

In certain cases, the microstructure of the compositions and frits was studied on a Philips scanning electron microscope. Certain phase compositions were analysed with an

energy-dispersive X-ray analysis (EDXA) instrument hooked up to an electronic microscope.

With a view to analysing the effect of given frits on sealed porosity, test specimens fired at temperatures close to maximum densification temperature were examined with an optical microscope, after polishing these with progressively finer grained abrasive (first with silicon carbide, then with diamond and finally with abrasive having a mean grain size of 1 µm).

*Colour development*

To determine the influence of the frit on colour development, coloured compositions were prepared by adding 1.0 % of a blue pigment.

The compositions were prepared by wet mixing the pigment with blends of the porcelain tile body and frit in a planetary mill for 10 min. Specimens were subsequently formed and fired according to the methods set out above, determining their bulk density and chromatic coordinates.

**4. RESULTS**

The results are discussed below. First, the results are discussed relating to the preliminary tests run to select the most appropriate frits for developing compositions with high meltability and whiteness. The mechanisms allowing the selected frits to provide the compositions with these properties are then discussed.

**4.1.- PRELIMINARY TESTS**

***4.1.1.- Selection of the most suitable frits for developing compositions with high meltability***

Figure1 presents the vitrification diagrams of the test compositions. The diagram corresponding to the STD composition is also included to facilitate the observation of the arising changes. These have been used to calculate working or maximum densification temperature (Tmax) for each composition, as well as the specimen properties at these temperatures: bulk density (Dmax), linear shrinkage (L.S.), water absorption (W.A.) and chromatic coordinates (L\*, a\* y b\*). The data are presented in Table 2. The values of parameters ΔT and ΔR are also included, which represent the firing range of each composition. ΔT corresponds to the temperature range at which fired bulk density does not vary more than 0.01g/cm<sup>3</sup> in respect of peak value and ΔR was calculated from the difference between the ΔT values of the frit-containing compositions and that of the STD composition from the following equation:

$$\Delta R = \frac{(\Delta T - \Delta T_{STD})}{\Delta T_{STD}} \cdot 100$$

	$T_{max}$ (°C)	$D_{max}$ (g/cm <sup>3</sup> )	W.A.(%)	L.S.(%)	$L^*$	$a^*$	$b^*$	$\Delta T$ (°C)	$\Delta R$ (%)
STD	1212	2.42	< 0.1	8.0	71.9	1.6	12.6	31	-
CA	1191	2.41	< 0.1	8.0	72.2	1.8	12.9	21	-32
CB	1188	2.40	< 0.1	7.8	72.8	1.8	12.8	16	-48
CC	1154	2.41	< 0.1	8.0	71.4	2.0	12.2	33	+6

**Table 2.**  
Composition  
maximum  
densification  
temperature and  
specimen  
properties at this  
temperature.

It can be observed that in general, adding transparent frits to the porcelain tile composition produced a drop in peak densification temperature (between 20°C and 60°C) and a narrower firing cycle, while the magnitude of both effects depended on the frit involved. Frit C was an exception to this behaviour, as it noticeably lowered firing temperature without narrowing the firing range.

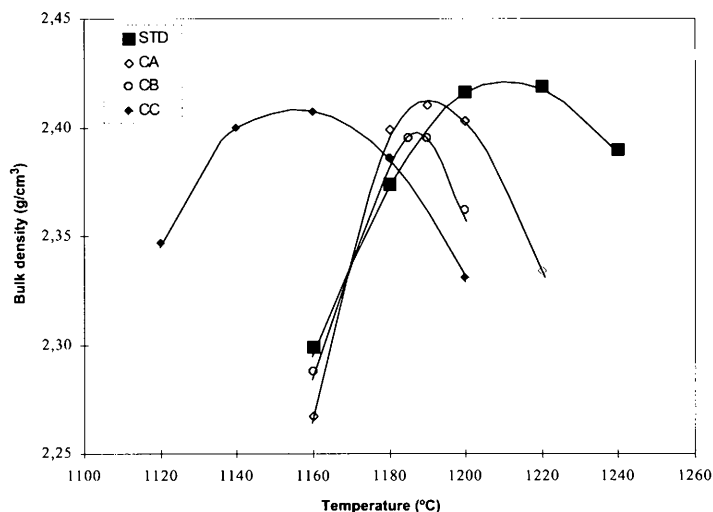


**Figure 1.** Vitrification diagrams of the compositions containing fluxing frits.

The effects mentioned above (lower  $T_{max}$  and higher  $\Delta T$ ) are due on the one hand to the lower melting temperature of the frits, and on the other, to the drop in liquid-phase viscosity as a result of the incorporation of certain cations present in the frits (Na, K, B, etc.)<sup>[1, 2, 3]</sup>. Thus, the composition made up with frit B, containing 6.6 wt% alkali oxides, exhibited lower values for  $T_{max}$  and  $\Delta T$  than the composition with frit A, with 3.7 wt% alkali oxides.

However, the most interesting feature was the apparently opposite effect of the sharp fall in maximum densification temperature and slight broadening of the firing range produced by frit C. The thermal behaviour of this frit differed from that of the others, as during firing, instead of producing transparent glazes, it gave rise to semi-transparent, matt glazes. Moreover, assuming that the frit melted during firing of the porcelain tile bodies, which was not verified, the presence of lithium in the liquid phase would lower its viscosity<sup>[4]</sup>. The behaviour of this composition can therefore not be explained just on the basis of the modification of liquid-phase viscosity, but also involves other liquid-phase characteristics, such as surface tension.

Thus, analysis of the findings indicates that the most appropriate tested frit for

- [1]. ENDELL, K.; HELLBRÜGGE, H. *Über den Einfluss des Ionenradius und der Wertigkeit der Kationen auf den Flüssigkeitsgrad von Silicatschmelzen*. *Angew. Chem.*, 53, (25-25), 271-273, 1940.
- [2]. SHARTIS, L.; SPINNER, S.; CAPPS, W. *Density, expansivity and viscosity of molten alkali silicates*. *J. Am. Ceram. Soc.*, 35(6), 155-160, 1952.
- [3]. BRÜCKNER, R.; FERNÁNDEZ NAVARRO, J.M. *Physikalisch-chemische Untersuchungen in System B<sub>2</sub>O<sub>3</sub>-SiO<sub>2</sub>*. *Glastechn. Ber.*, 39(6), 283-293, 1996.
- [4]. SHARTIS, L.; CAPPS, W.; SPINNER, S. *Viscosity and electrical resistivity of molten alkali borates*. *J. Am. Ceram. Soc.*, 36(10), 319-326, 1953.

developing highly meltable compositions is frit C, as this frit produced the greatest drop in firing temperature without narrowing the working temperature range.

**4.1.2.- Selection of the most suitable frits for developing compositions with high whiteness**

Figures 2 and 3 present the vitrification diagrams corresponding to the two groups of tested compositions. As in the foregoing point, these diagrams were used to calculate test specimen maximum densification temperatures and properties at this temperature (Table 3).

As in the foregoing section, it can be observed that adding opaque frits to the porcelain tile composition led to a drop in maximum densification temperature and a narrower firing range, the magnitude of both effects depending on the frit used. These effects, as already mentioned, were due to the lower melting temperature of the frits and reduction in liquid-phase viscosity in the bodies. This can be clearly observed in the case of frit G, which on containing a high percentage of PbO, noticeably lowered maximum densification temperature besides being one of the compositions with the narrowest working range.

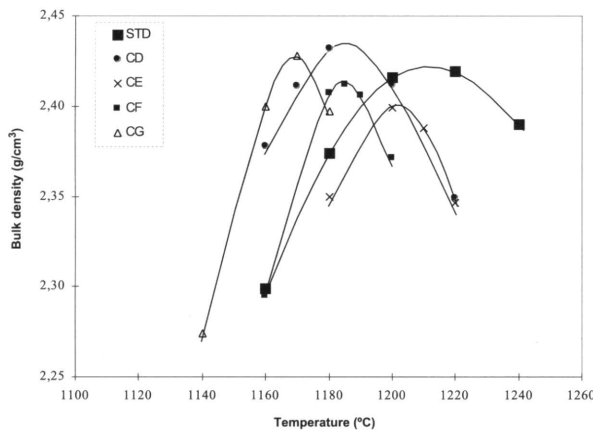


Figure 2. Vitrification diagrams of the zirconium-containing compositions.

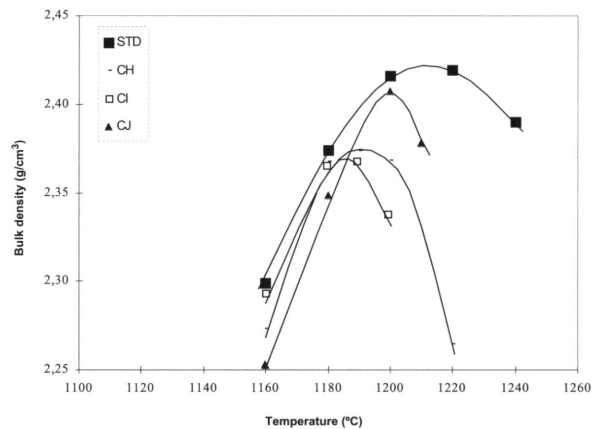


Figure 3. Vitrification diagrams of the zirconium-free compositions.

	T <sub>max</sub> (°C)	D <sub>max</sub> (g/cm <sup>3</sup> )	W.A.(%)	L.S. (%)	L*	a*	b*	ΔT(°C)	ΔR(%)
STD	1212	2.42	< 0.1	8.0	71.9	1.6	12.6	31	-
CD	1184	2.43	< 0.1	8.2	73.9	1.5	11.3	20	-35
CE	1201	2.40	0.0	7.8	72.6	1.7	13.1	13	-58
CF	1185	2.41	0.0	8.0	73.7	1.6	12.1	11	-65
CG	1170	2.43	< 0.1	8.1	74.2	1.8	12.2	13	-58
CH	1190	2.37	< 0.1	7.2	72.7	1.6	13.1	23	-26
CI	1185	2.37	0.0	7.4	74.4	1.6	17.2	18	-42
CJ	1200	2.41	< 0.1	7.7	74.1	1.6	12.5	13	-58

Table 3. Composition maximum densification temperature and test specimen properties at this temperature.

With regard to fired specimen whiteness, it should be noted that this also appears to depend on the nature of the frit used. Thus, all the compositions to which frit was added exhibited greater whiteness than the STD composition, basically detected by the rise in the value of the  $L^*$  coordinate. This suggests that crystalline-phase devitrification occurs during specimen firing, which is responsible for raising fired product whiteness. Thus, while in the case of frits D, E, F and G, the devitrifying phase will be zircon, in frits H, I and J, devitrification will respectively be diopside, sphene and celsian.

Frits D, F, G, I and J produced the greatest rise in the  $L^*$  coordinate. Of these, the most appropriate one for use in compositions with high whiteness is frit D, as this noticeably raised fired product whiteness, without excessively narrowing the firing range, or significantly raising fired product porosity. The other frits were discarded for the following reasons:

- Frits F, G and J. Although some of these frits produced even higher degrees of whiteness than frit D, they appreciably narrowed the firing range, which would worsen tile behaviour during this stage.
- Frit I. Incorporating this frit did not excessively narrow the firing range, but it raised the yellowish hue of the body, revealed by the high value of coordinate  $b^*$  ( $b^* < 0$  blue,  $b^* > 0$  yellow), while also raising body porosity.

## 4.2.- STUDY OF THE CC COMPOSITION

In order to determine the reasons for the simultaneous rise in meltability and firing range on adding frit C to the STD composition, frit C firing behaviour and that of the composition with frit C (CC) were studied separately. Melting tests were run for this purpose on a hot-stage microscope, and the appearance of the test specimens was examined by electron microscopy at different temperatures, determining the crystalline phases present by X-ray diffraction (XRD).

### 4.2.1.- Frit C

The findings are presented in Figures 4 to 8. Figure 4 shows the variation of frit shrinkage with temperature during the fusion test. It can be observed that at very low temperatures of around 610°C, the frit starts shrinking, which stops over a wide range of temperatures (650°C-850°C). This behaviour can be associated with devitrification in this temperature range, which raises the body's apparent viscosity to the point of completely arresting the sintering process that had initiated.

Figure 5 presents a picture of the frit fired at 750°C, which lies within the range mentioned. Frit particles were found welded together by small menisci (a) of liquid phase, which together with the rounded shape of some frit particles, indicates sintering process start. A change in colour can also be observed in certain frit particle regions,

indicating a change in chemical composition. Thus, while the grey areas (b) exhibit a composition only made up of Si, Al and O, the white areas (c) contain, Na, Ca, K and small proportions of Fe and Ti besides these elements. As this technique does not allow identifying lithium, XRD scans were run, detecting spodumene as the only crystalline phase present in the sample. Thus, during frit firing, spodumene ( $\text{LiO}_2 \cdot \text{Al}_2\text{O}_3 \cdot 4\text{SiO}_2$ ) devitrifies at around 650°C, producing a grey colour in the images, and liquid phase forms of composition Si, Al, O, Na, Ca and K, producing a white colour in the image.

The sintering process continues above 850°C (Figure 4), almost stopping at around 980°C. This is confirmed in Figure 6, which depicts the appearance of the frit at 940°C. The figure shows that most of the (black-coloured) pores initially present in the specimen have been eliminated and also shows the presence of a high quantity of spodumene crystals (grey colour, b) with a mean size of 3  $\mu\text{m}$ , cemented by white-coloured liquid phase (c), with a very similar composition to that found at 750°C.

Between 980°C and 1050°C, the specimen continues to shrink, however at a slower rate. This change in sintering rate stems from the lower remaining porosity in the specimen and from the presence of trapped gases in the closed pores. Figure 7 presents the appearance of a specimen fired in this temperature range. The specimen exhibits high densification with spherical

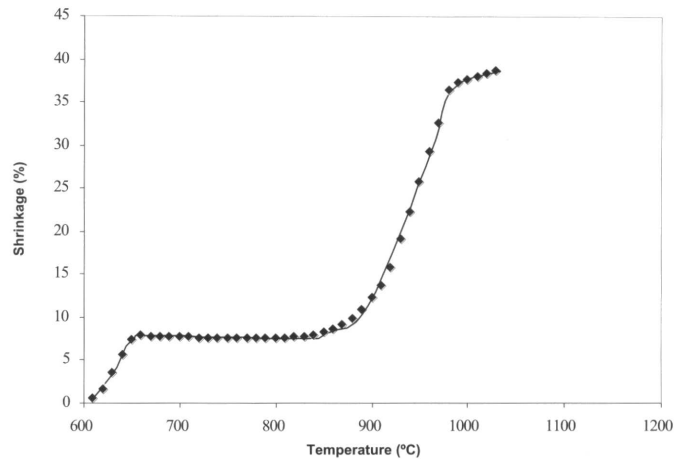


Figure 4. Frit C sintering curve.

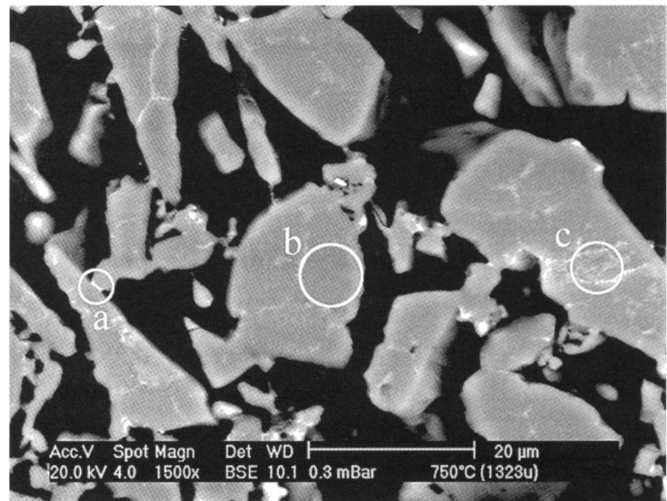


Figure 5. Micrograph of frit C (T=750°C)

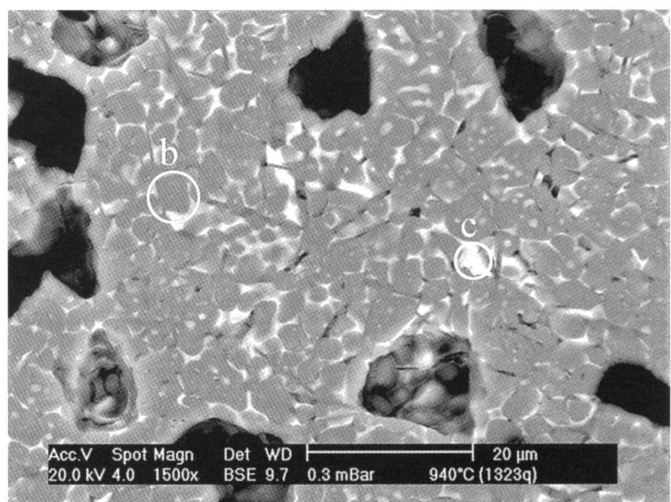


Figure 6. Micrograph of frit C (T=940°C)

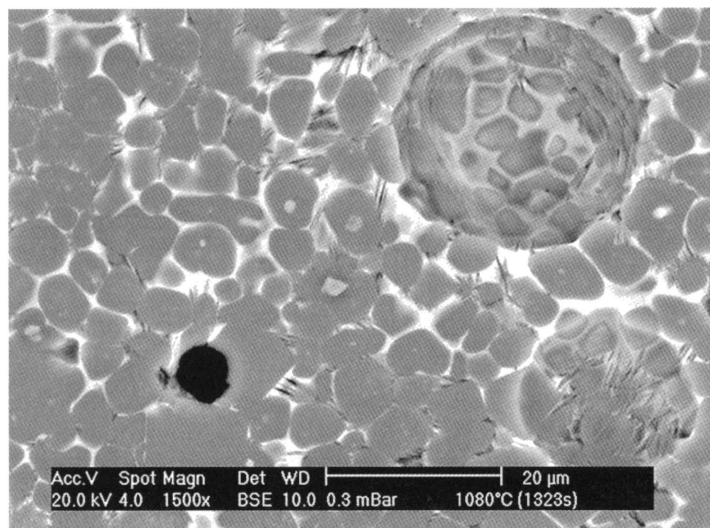


Figure 7. Micrograph of  
frit C ( $T=1050^{\circ}\text{C}$ )

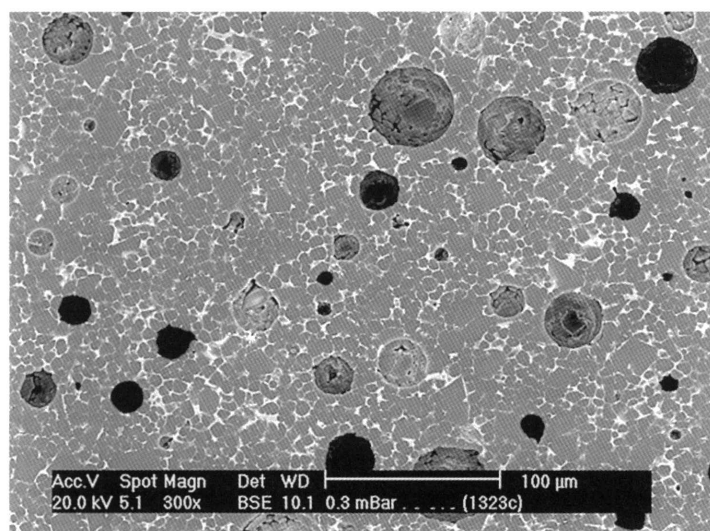


Figure 8. Micrograph of  
frit C ( $T=1154^{\circ}\text{C}$ )

pores, characteristic of the final stages of the sintering process. Spodumene crystal growth is also detected, with a mean crystal size of about  $8\ \mu\text{m}$ .

Finally, a frit specimen was examined, fired at the temperature at which the CC composition attains maximum densification ( $1154^{\circ}\text{C}$ ). The corresponding image (Figure 8) shows the presence of a high proportion of spodumene crystals, which are welded together by low-viscosity liquid phase, judging by the spherical shape of all the pores present. Spodumene crystal growth has reached the point at which these crystals exhibit a mean size of around  $10\ \mu\text{m}$ .

Summing up, it can be concluded that during frit C heat treatment, spodumene devitrifies at relatively low temperatures ( $650^{\circ}\text{C}$ ), with subsequent crystal growth as temperature rises. At composition CC firing temperature ( $1154^{\circ}\text{C}$ ), these crystals exist together with a small proportion of liquid phase consisting of Si, Al, O, Na, Ca and K.

#### 4.2.2 Composition CC

Figure 9 plots the sintering curves of the STD and CC compositions. They show that the presence of frit C produces the following effects:

- Left shift of the shrinkage-temperature curve, indicating that the sintering process starts at considerably lower temperatures ( $1100^{\circ}\text{C}$  for the STD and  $1060^{\circ}\text{C}$  for the CC composition).
- Rise of sintering rate (curve slope).
- Considerable decrease of bloating or maximum densification temperature without narrowing the firing range.

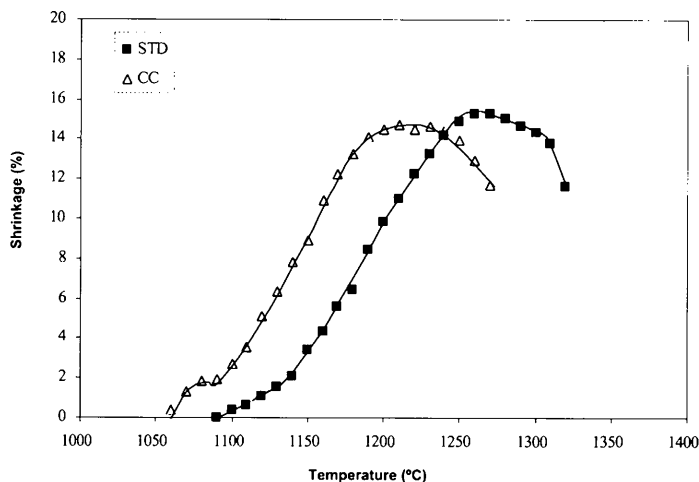


Figure 9. STD and CC composition sintering curves.

The melting test outcomes (Figure 9) confirm the findings set out in point 4.1, i.e., adding frit C lowered firing temperature without narrowing the firing range. However, these results cannot be explained on the basis of the behaviour observed above for this frit, as spodumene devitrifies during firing, which is a highly refractory crystalline phase at porcelain tile firing temperatures.

With a view to establishing whether there was any difference in frit C firing behaviour when the frit was a porcelain tile composition constituent, specimens of the CC composition were examined by electron microscopy at different firing temperatures (800, 1000, 1025, 1050, 1075 and 1100°C). Figures 10 to 15 present representative images of the specimens at these temperatures.

At low temperatures (800°C), when porcelain tile sintering has not yet started, the frit particles exhibit a very similar appearance to those shown in Figure 5, i.e., a characteristic change of colour in some regions, indicating that spodumene crystallisation has already begun (Figure 10). This was confirmed by XRD. On raising the temperature (1000°C), the change in colour became more pronounced, coinciding with massive spodumene crystal devitrification in the frit particles (Figure 11). The sintering start of the porcelain tile composition can also be observed, revealed by the presence of numerous particles joined by small menisci.

On reaching 1025°C, liquid phase has clearly started to develop, mainly stemming from the progressive melting of feldspar. In the corresponding image (Figure 12), this liquid phase starts interacting with the frit particles, which still exhibit a well-defined surface. On raising temperature, liquid-phase development becomes greater, producing frit integration in the melt (Figure 13). However, frit particle surfaces can still be distinguished, albeit less sharply. The process continues until above 1100°C (Figure 15) the frit particles can no longer be identified, either visually or by point microanalysis.

It can therefore be inferred that the presence of frit C did not modify the behaviour of the porcelain tile compositions during firing until reaching 1025°C, as no type of interaction between the frit particles and the other compositional components was detected. Above this temperature, the numerous spodumene crystals existing in the frit

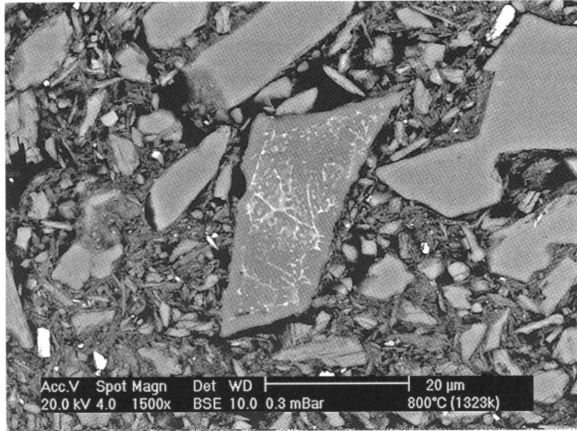


Figure 10. Micrograph of the CC composition at 800°C.

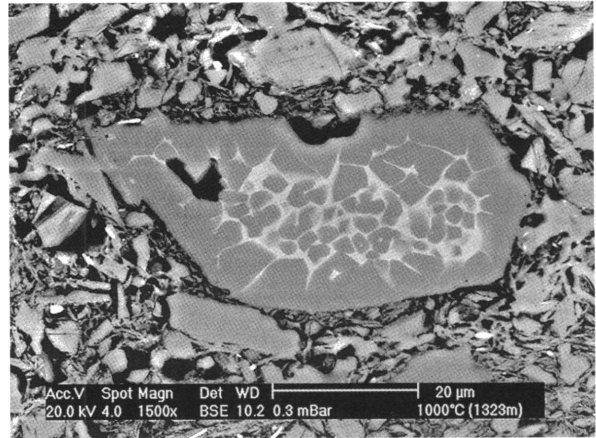


Figure 11. Micrograph of the CC composition at 1000°C.

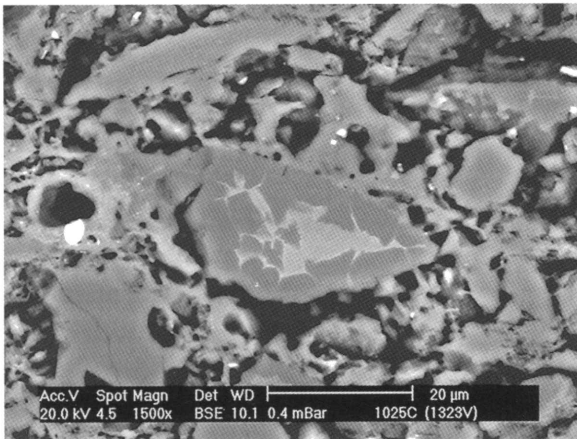


Figure 12. Micrograph of the CC composition at 1025°C.

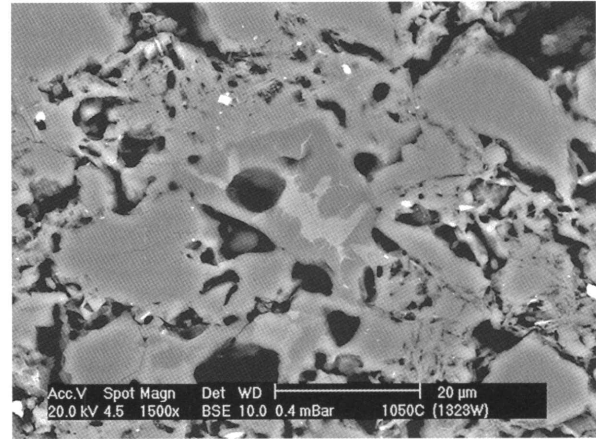


Figure 13. Micrograph of the CC composition at 1050°C.

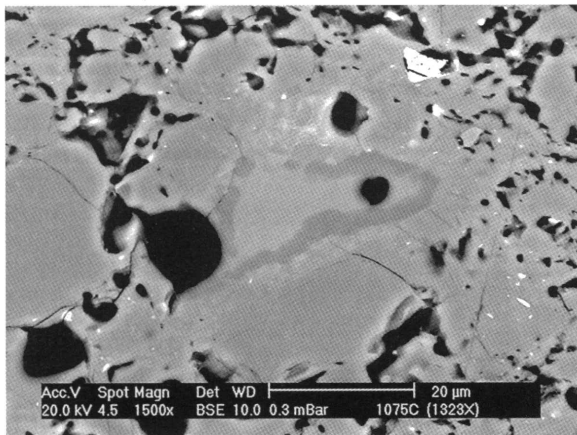


Figure 14. Micrograph of the CC composition at 1075°C.

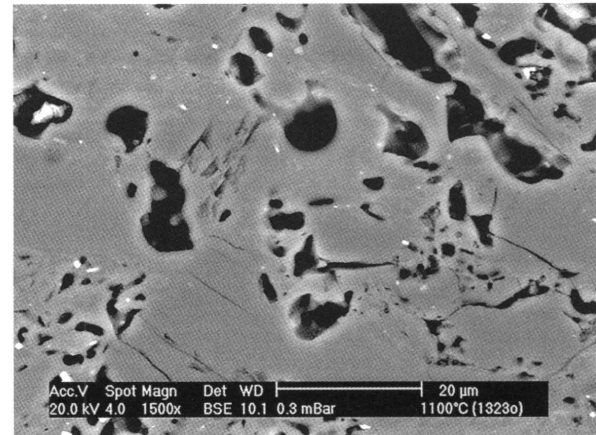


Figure 15. Micrograph of the CC composition at 1100°C.

particles started integrating in the liquid phase of the body, modifying liquid-phase quantity and chemical composition, which basically became richer in lithium.

The rise in the proportion of liquid phase, as well the change in liquid-phase chemical composition could alter the way the sintering process develops, as these changes modify liquid-phase surface tension and viscosity. Thus, porcelain tile sintering rate ( $d\epsilon/dT$ ) depends, amongst other factors, on liquid-phase viscosity and capillary pressure according to the following relation <sup>[5]</sup>:

$$-\frac{d\epsilon}{dT} \propto \frac{(P_c - P_g)}{\eta} \quad P_c = \frac{2 \cdot \gamma}{r}$$

where:

- $\epsilon$ : tile porosity
- T: temperature
- $P_c$ : capillary pressure
- $P_g$ : pressure of the trapped gases in the closed pores
- $\gamma$ : surface tension
- r: pore radius
- $\eta$ : effective viscosity of the solid+liquid system

In the starting stages of the sintering process, closed porosity is much lower than opened porosity or even zero. The assumption can therefore be made that the effect of gas pressure inside the pores on sintering rate is negligible with regard to capillary pressure ( $P_g \ll P_c$ ). Hence, sintering rate will be a function of liquid-phase surface tension and the body's effective viscosity. The presence of lithium in the liquid phase modifies its characteristics, lowering liquid-phase viscosity and raising its surface tension <sup>[6]</sup>. Both effects raise the sintering rate, explaining the behaviour observed in the vitrification diagrams and in the melting tests.

In the final sintering stages, which coincide with porcelain tile firing temperatures, most of the porosity in the body is sealed porosity, so that gas pressure in the pores is no longer negligible. Raising temperature increases trapped gas pressure, reducing sintering rate until this cancels out when gas pressure equals capillary pressure. From this moment onwards, raising temperature makes  $P_g > P_c$ , increasing sealed pore size, a phenomenon that causes bloating. The wider or narrower firing range of the materials will therefore depend on the relative variation of  $P_c$  and  $P_g$  with firing temperature.

The pressure of the gases trapped in the pores depends linearly on firing temperature. This variation should therefore not alter significantly with the compositional change. However, the capillary pressure of the liquid phase corresponding to the CC composition, as mentioned above, will be higher, affording greater resistance to the pressure of the gases trapped in the pores, and consequently, slowing down bloating.

[5]. ORTOS TARI, M. J. *Sinterización de piezas de pavimento gresificado*. Valencia: Universidad de Valencia, 1991. Tesis Doctoral.  
 [6]. SHARTIS, L.; SPINNER, S. *Surface tension of molten alkali silicates*. J. Res. Nat. Bur. Stand., 46(5), 385-390, 1951.

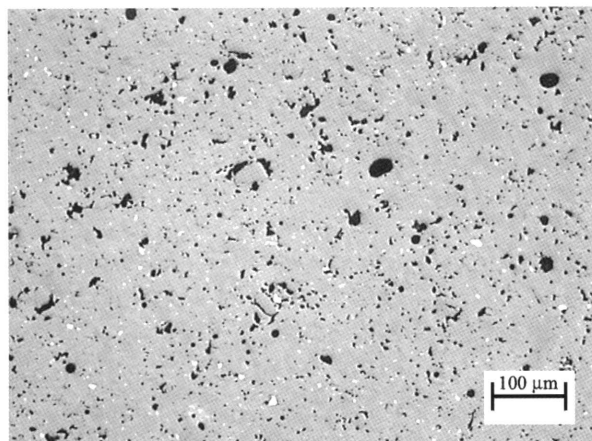


Figure 16. Appearance of the STD composition.

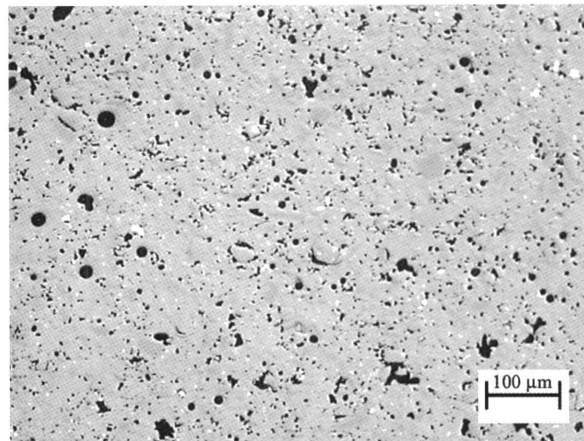


Figure 17. Appearance of the CC composition.

#### 4.2.3.- Study of certain fired product properties

To round off this part of the study, it was considered convenient to determine whether the presence of the frit modified fired product properties. The studied properties were body porous structure, because of its close relationship with fired tile stain resistance, and the colour development capability.

##### *Fired body microstructure*

The microstructure of polished cross sections of specimens fired at temperatures approaching maximum densification was examined by optical microscopy. Figures 16 and 17 present images of representative regions of the specimens made with the STD and CC compositions. They show that for the tested porcelain tile composition, a 6% addition of frit C did not significantly affect the proportion or size of the pores present in the resulting material. These findings matched the scarce variation in bulk density found in point 4.1.

As the 6% frit addition did not noticeably alter specimen porous structure, the stain resistance of the polished product will foreseeably also remain unaffected.

	Non-coloured compositions		Coloured compositions	
	STD	CC	STD	CC
L*	71.9	71.4	52.0	51.6
a*	1.6	2.0	-4.4	-5.8
b*	12.6	12.2	-9.6	-12.9

Table 4. Colour development.

##### *Colour development*

Table 4 details the chromatic coordinates of the coloured and non-coloured STD and CC compositions at maximum densification temperature.

For the compositions coloured with the blue pigment, the most significant coordinates are b\*, indicating blueness, and L\*, which provides information on colour

intensity. Though incorporating frit C did not significantly modify the value of the L\* coordinate, it produced more b\* coordinate negative values, indicating that the resulting colour exhibited greater blueness. The values for coordinate a\* also dropped slightly, so that the colour produced had a slightly greater greenness.

The greater capacity of composition CC to develop blueness could be due to the rise in the proportion of glassy phase in the bodies on adding frit C. It was thus found that at temperatures above 1025°C, frit C integrated in the existing liquid phase, hence raising the liquid-phase proportion. This fact should increase the transparency of the resulting bodies and therefore improve the yield of the added body stains.

#### 4.3.- STUDY OF THE CD COMPOSITION

As in the foregoing point, to determine the causes of the rise in whiteness in composition CD compared to composition STD, frit behaviour was studied first and subsequently that of the CD composition.

##### 4.3.1.- Frit D

Figure 18 plots the frit sintering curve. Shrinkage can be observed to commence at temperatures of around 830-840°C, stabilising in the range 950-1030°C and ending at about 1080°C. Shrinkage stabilisation across the 980 to 1030°C temperature range is due to zircon devitrification. According to the literature <sup>[7]</sup>, this crystalline species devitrifies at temperatures approaching 1000°C, generating a crystalline structure in the liquid matrix, which raises the viscosity of the material, thus arresting the sintering process. Subsequent shrinkage arises when the viscosity of the liquid phase has decreased enough to start a sintering process by the collapse and partial dissolution of the crystalline structure.

Zircon devitrification was confirmed by XRD analysis of the frit specimen in which this crystalline species was identified. Figure 19 shows a picture of the frit specimen fired at 1184°C, maximum densification temperature of the CD composition. At these temperatures the frit had fully melted, and white particles can be observed, whose composition was made up of Si, Zr and O. This confirmed zircon devitrification during firing.

##### 4.3.2.- CD composition

To verify whether the increased whiteness of composition CD compared to composition STD was due to zircon devitrification from the frit, XRD scans were run on specimens of both compositions fired at temperatures close to maximum densification. Three crystalline phases were identified in the STD composition: quartz, albite and

[7]. MORENO BERTO, A. *Estudio de la formación de fases cristalinas en vidriados blancos de circonio. Factores que influyen sobre su índice de blancura*. Valencia: Universidad de Valencia, 1994. Tesis Doctoral.

mullite. In composition CD, besides these three phases, zircon was also identified. To confirm the presence of zircon, a CD specimen fired at 1184°C was examined by scanning electron microscopy. The corresponding images are shown in Figures 20 and 21. The micrograph in Figure 20, taken at a smaller magnification, shows regions of white particles, identified by EDXA as zircon, which appeared to correspond to the areas in which the frit particles were originally found. This phenomenon can be more clearly observed in the second micrograph, in which zircon crystals can be observed (white, needle-like particles), forming a kind of frame containing a lighter-coloured region, identified by microanalysis as glassy phase from frit fusion. This confirms the data found in the literature [8], according to which zircon devitrification takes place by surface and not by mass devitrification, which is why crystals form at the frit particle surface.

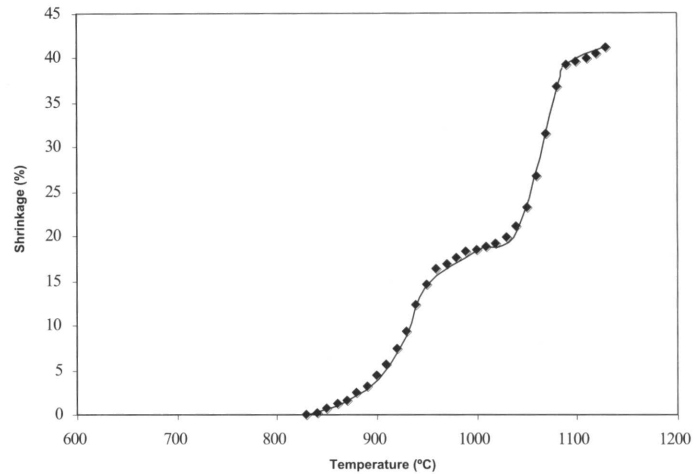


Figure 18. Frit D sintering curve.

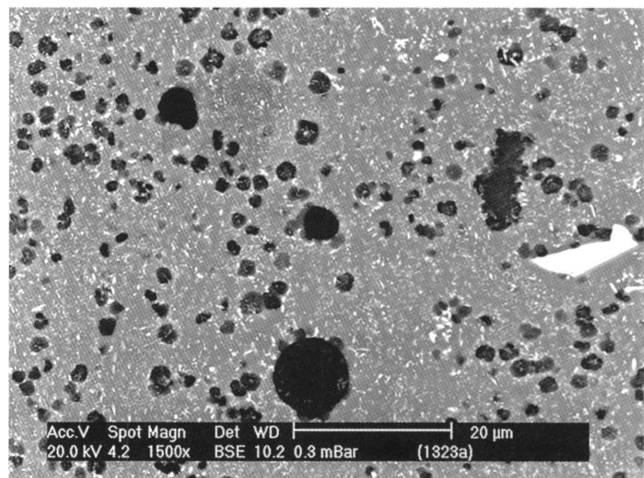


Figure 19. Micrograph of frit D.

#### 4.3.3.- Study of certain composition properties

##### *Microstructure of the resulting materials*

Figures 22 and 23 present images of the microstructures produced in composition STD and CD specimens. The presence of frit D in the added percentage did not alter the porous structure of the resulting material, so that polished product behaviour with regard to stain resistance should not significantly change.

##### *Colour development*

The values of the chromatic coordinates of the coloured and non-coloured STD and CD compositions are presented in Table 5. For the non-coloured CD composition, zircon devitrification from frit D particles, confirmed in the foregoing point, produced a rise in

[8]. ESCARDINO, A.; MORENO, A.; AMORÓS, J.L.; GOZALBO, A.; APARICI, J.; SÁNCHEZ, L.E. Estudio de la formación de fases cristalinas en vidriados blancos de circonio. *Técnica Cerámica*, 242, 217-229, 1996.

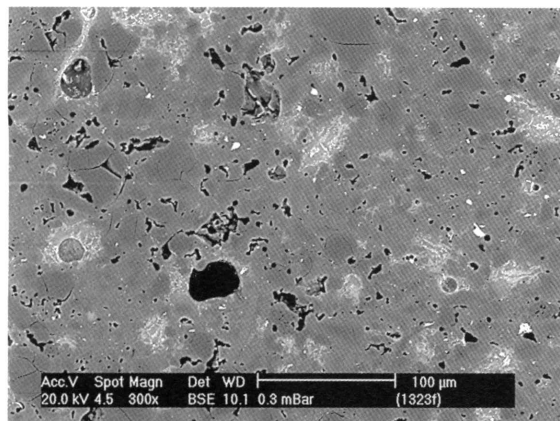


Figure 20. Micrograph of composition CD

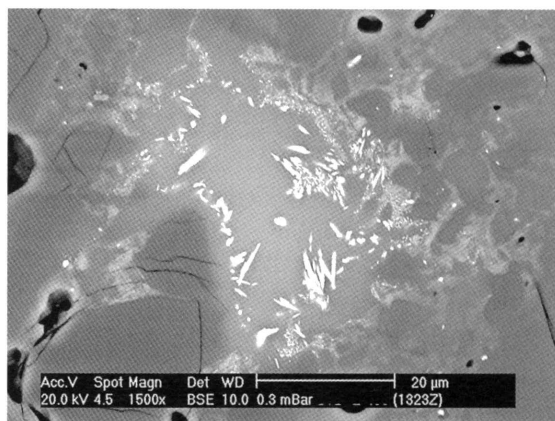


Figure 21. Micrograph of composition CD

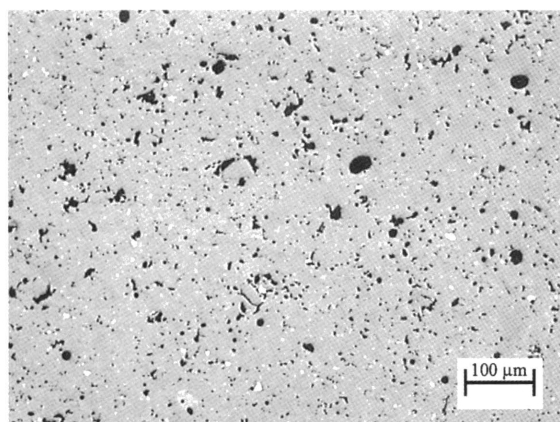


Figure 22. Appearance of composition STD

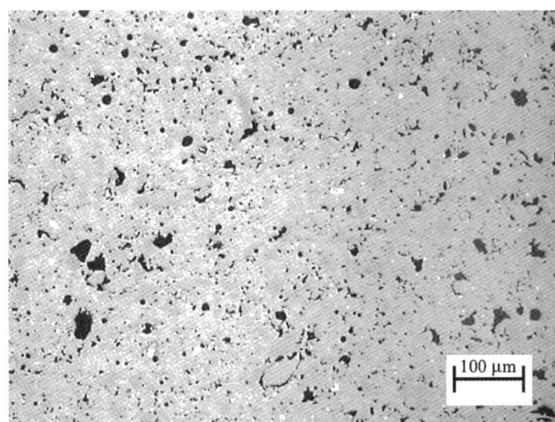


Figure 23. Appearance of composition CD

	Non-coloured compositions		Coloured compositions	
	STD	CD	STD	CD
L*	71.9	73.9	52.0	52.7
a*	1.6	1.5	-4.4	-6.1
b*	12.6	11.3	-9.6	-13.2

Table 5. Colour development.

the whiteness of the resulting bodies owing to the opacifying effect of this crystalline phase. This yielded higher coordinate L\* values and a lower coordinate b\* value.

When blue pigment was added to both compositions, the frit-containing composition yielded greater blueness, as the value of the b\* coordinate was more negative. This improvement is to be associated on the one hand with the lower coordinate b\* of the non-coloured CD composition, i.e., a less yellow starting composition was involved. On the other hand, as shown in the foregoing point, besides devitrifying zircon crystals, the frit also produces a certain quantity of liquid phase, which is responsible for the greater meltability of this composition. This last effect could slightly raise the transparency of the bodies and hence encourage development of the blue colour.

## 5. CONCLUSIONS

The following conclusions can be drawn from the study:

- The use of frits as fluxing raw materials in porcelain tile compositions permits lowering the firing temperature of these products, although it also narrows the firing range in most cases.
- As an exception to this behaviour it was found that the use of a frit that contributed lithium to the composition noticeably reduced porcelain tile firing temperature, without lowering the firing range. The modification of the physical properties of the arising liquid phase in the materials in the firing stage appears to be responsible for this behaviour.
- The use of frits devitrifying crystalline phases during porcelain tile firing can serve to raise porcelain tile whiteness. Of these frits, the ones devitrifying zircon are the most interesting, owing to the enhanced whiteness they provide. This effect could serve as an alternative procedure to using zircon as an opacifying raw material. The smaller size of the devitrifying zircon particle encourages the opacifying effect of this crystalline phase, which could entail a technical advantage compared to using zircon admixtures.
- In the tested percentage, the two studied frits (frits C and D) did not noticeably modify the characteristics of the fired product (shrinkage, porous structure, etc.), except for colour development, which improved appreciably owing to the greater glassy phase arising in the bodies.